STP-DEQ-Net: A Deep Equilibrium Model Based on ISTA Method for Image Compressive Sensing

Youhao Yu[1,2], Richard M. Dansereau[1]
Department of Systems and Computer Engineering, Carleton University, Ottawa, Canada[1]
School of Information Engineering, Putian University, Fujian, China[2]
youhaoyu@sce.carleton.ca rdanse@sce.carleton.ca

***Abstract*—With the aim of finding a compact and efficient model for compressive sensing (CS) imaging, we sample images based on semi-tensor product (STP) and design a deep equilibrium (DEQ) neural network. We measure the images and produce their initial reconstruction with STP method. The results can be refined by deep unrolling methods (DUMs) which use architectures borrow insights from iterations of an optimization method. Though DUMs have well-defined interpretability, a few iterations will make the model takes up huge memory space. It is difficult for training and application. Inspired by the iterative shrinkage-thresholding algorithm (ISTA) and deep equilibrium architecture, we build a deep network dubbed as STP-DEQ-Net. It reduces the storage of the system from multiple ISTA iteration blocks to only one block. The experiments show that the proposed method operates with attractive performance compared with competing methods. The trained model has trade-offs between reconstruction quality and computation.**

Keywords—compressive sensing, semi-tensor product, ISTA, deep equilibrium model, image reconstruction

I. INTRODUCTION

Compressive sensing (CS) is a signal acquisition and reconstruction method [1]–[3]. It reconstructs the original signal that is sparse in a transform domain from far fewer measurements than required by the Shannon-Nyquist sampling theorem [4]. A signal $x \in \mathbb{R}^N$ is sparse in some domain if

$$s = \Psi x \tag{1}$$

where $\Psi \in \mathbb{R}^{N\times N}$ is a sparsifying orthonormal basis and the number of non-zero elements in $s \in \mathbb{R}^N$ is much less than N [3]. According to CS theory, the signal x qualifies for CS and can be sampled as

$$y = \Phi x \tag{2}$$

where $y \in \mathbb{R}^M$ is the measurement vector and $\Phi \in \mathbb{R}^{M\times N}$ ($M<N$) is a suitable measurement matrix that should satisfy the restricted isometry property (RIP) [5]. CS has many potential applications, such as radar signal sampling[6], cryptosystem [7], magnetic resonance imaging (MRI) [8], video sensing [9], and snapshot imaging [10].

Since natural images are usually sparse in some domain (e.g., frequency domain), in CS-based image compression an image can be sampled and compressed by encoding the image with linear measurements like in (2). Traditional CS-based methods usually formulate signal reconstruction as a convex optimization problem [11]. As such, the original image can be reconstructed by an iterative optimization technique. Although algorithms usually have convergence guarantees, the iteration process is computationally expensive. Compared to optimization based methods, neural network (NN) based reconstruction algorithms have been shown to alleviate the computational cost with reasonable performance [12]. NN models directly learn the inverse mapping from the measurements to the original signals. The measurement matrix Φ can also be acquired through training [13].

Many NNs have studied CS measurement reconstruction. Most of the models work like a black box, which in the sense that while they can approximate some function, studying their structure won't give insights on the structure of the function being approximated. Different from other NNs operating like black boxes, optimization-inspired deep unrolling methods not only allow for interpretability in its network design, but also have excellent performance [14]. Deep unrolling includes repeated blocks with identical architectures. Deep unrolling methods are flexible since they work by learning, allow for structural diversity, and have architectures that simulate a fixed number of optimization iterations. However, the number of iterations must be small since a large model is difficult to train and has higher computational requirements. To simplify the structure, deep equilibrium (DEQ) architectures for inverse problems use fixed point iteration [15], [16] and only needs one iteration structure unlike deep unrolling. Also, the computational budget can be set at test time since reconstruction accuracy improves consistently with repeated application of the fixed-point iteration [16].

In the rest of this article, Sec. II presents related work. The measurement and initial reconstruction based on STP is introduced in Sec. III. ISTA algorithm and the proposed STP-DEQ-Net are discussed in Sec. IV. Sec. V gives experimental results of the proposed model and competing algorithms. Finally, conclusions are drawn in Sec. VI.

II. RELATED WORK

In [17], [18], STP is adopted and the iteratively re-weighted least-squares (IRLS) algorithm is used for image CS reconstruction. They have reasonable peak signal-to-noise ratio (PSNR) and structural similarity index (SSIM) at a high sampling rate (SR=M/N), but need many iterations and a forward/inverse wavelet transform is used before/after CS. In [19], STP is developed into an NN (called STP-Net) for image CS. STP-Net efficiently measures an image and provides a good initial reconstruction for subsequent models. It works like an autoencoder, and its initial value of learnable parameters corresponding to the measurement matrix satisfy RIP [5]. The data driven learning for the measurement matrix allows measurements to have more information even at low sampling rate. To reconstruct image details, especially in the case of low sampling rate, [20] propose a dual-path attention network (DPA-Net) for reconstructing high quality images that preserve texture details from the CS measurements. The network is a structure-texture representation model composed of a structure path, a texture path and a texture attention

module. Usually the performance of a model is greatly impacted by the features in the training dataset, the number of training samples and the correlation between the training samples and target image. In order to cope with this issue, a self-supervised Bayesian deep network (SSB-Net) was proposed which predicts the target image with uncertainty [21]. The uncertainty enables the reconstructed image with small mean squared error (MSE) by averaging multiple predictions. The model is trained without requiring any external training images. A diffractive sensing and complex-valued reconstruction network (DSCR-Net) is introduced in [22]. It employs light diffraction for efficient sampling and develops a complex-valued reconstruction network to facilitate reconstruction quality. In [23], a sampling and whole image denoising network based on generative adversarial network (GAN) is proposed (dubbed SWDGAN). A whole image dense residual denoising module is applied to remove block artifacts and enhance feature representation. To remove batch normalization (BN) artifacts, they do not use a BN layer. In the sampling process they apply a fully connected network, which has a lot of learnable parameters. For textured images, their reconstruction is excessively smooth. To improve the details, a parallel enhanced structure (PE-Net) is proposed in [24]. PE-Net includes a basic network for initial reconstruction and an enhanced network that learns details from the basic reconstruction and original image.

The aforementioned network-based CS methods adopt either repetitive convolutional or fully connected layers and lack a well-defined interpretability. Inspired by the iterative shrinkage-thresholding algorithm, ISTA-Net is proposed in [25]. ISTA-Net is a deep unrolling method with architecture that imitates a fixed number of iterations of traditional optimization methods to allow for interpretability in its design [14]. The network uses various structures inspired by insights of optimization-based methods in the CS domain [25]. ISTA-Net makes full use of the merits of network-based and optimization-based methods, but the number of iterations have to be quite small since a large model is difficult to train and has significant degradation if repeatedly applying ISTA-Net to implement more iterations [16].

In this paper, we propose STP-DEQ-Net. We build an ISTA iteration block as a DEQ model and connect it with STP-Net. STP-Net samples and compresses an image along rows and columns using semi-tensor product theory [19]. The sampling method provides a good initial reconstruction for subsequent deep equilibrium model. The model has fewer parameters to train and provides a theoretical foundation for the designed layer. The learnable parameters are learned end-to-end.

III. STP-NET

For network-based CS methods, block-based compressive sensing is widely used to reduce the complexity of CS measurement and reconstruction [26], [27]. For example,[20], [21], [23]–[25] all divide the original image into small blocks. For a large image, operations on small block can greatly reduce the number of parameters, which saves computational resources and memory usage. Then a fully connected layer can be used as measurement matrix for sampling.

However, block-based reconstruction methods ignore the dependence between adjacent blocks. The methods are usually plagued with serious blocking artifacts in the reconstruction, requiring additional denoisers [23]. STP-Net bypasses the

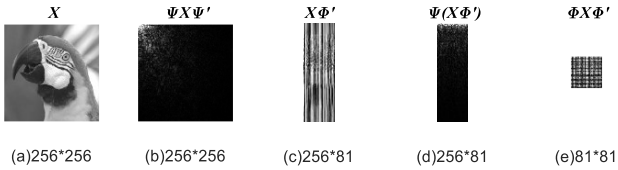

Fig. 1. Image measurements and sparsity [19]: (a) original image, (b) 1D sparsifying basis Ψ applied along columns and rows, (c) measure the image using random matrix Φ, (d) 1D sparsifying basis Ψ applied along columns of measurement, and (e) measure the image along columns and rows. Sampling rate = $(81/256)^2 \approx 10\%$.

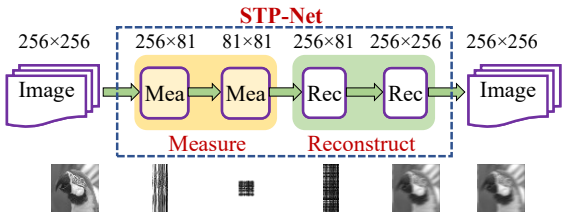

Fig. 2. STP-Net (Sampling rate≈ 10%) [19].

issue with semi-tensor product theory.

According to STP theory, a smaller measurement matrix $\Phi(t) \in \mathbb{R}^{M/t \times N/t}$ can be adopted, where t is a shrinkage factor that is a common divisor of M and N; $t < M$ ($M, N, t, M/t$ and N/t are all positive integers) [18], [28]. It has been proved in [18] that if $\Phi(t)$ satisfies RIP, then the STP between $\Phi(t) \in \mathbb{R}^{M/t \times N/t}$ and a sparsifying basis $\Psi \in \mathbb{R}^{N \times N}$ is still RIP. Compared with traditional methods, the size of the measurement matrix is shrunk by $1/t^2$. Different values of t may cause PSNR to decrease, but the maximum drop is no more than 5% [18]. Without partitioning image into blocks that introduces block artifacts, it provides good initial reconstruction for subsequent networks.

As shown in Fig. 1, it is visually apparent that the natural image in Fig. 1(a) can be sparse in some transform domain since Fig. 1(b) only has few white areas in the upper left corresponding to large amplitudes. Fig. 1(c) shows the measurement of the image along rows using a random matrix. After applying a 1D sparsifying basis along the columns, Fig. 1(d) shows the measurement along rows is still sparse in the transform domain since the large amplitudes are at the top. An image can be CS measured as (3) and shown in Fig. 2 for STP-Net.

$$Y = \Phi_1(t) \cdot X \cdot \Phi_2(t)^T \tag{3}$$

where $X \in \mathbb{R}^{N \times N}$ is the original image without segmentation and vectorization. $\Phi_1(t)$ and $\Phi_2(t)$ are the two small measurement matrix which can be same.

For block-based CS methods, an image $X \in \mathbb{R}^{256 \times 256}$ is usually cropped into many blocks, such as with size 33×33 [20], [21], [25]. The blocks are vectorized as a vector $x \in \mathbb{R}^{1089 \times 1}$. If sampling rate is 10%, the measurement matrix size should be 109×1089. According to STP-Net, there can be two measurement matrices with same size 81×256. It only needs less than 35% memory space of the former. The two matrices can even be the same. So, STP-Net saves space and is easier to train.

IV. PROPOSED STP-DEQ-NET FOR CS

In this section, we discuss traditional ISTA optimization for image CS reconstruction and the proposed STP-DEQ-Net.

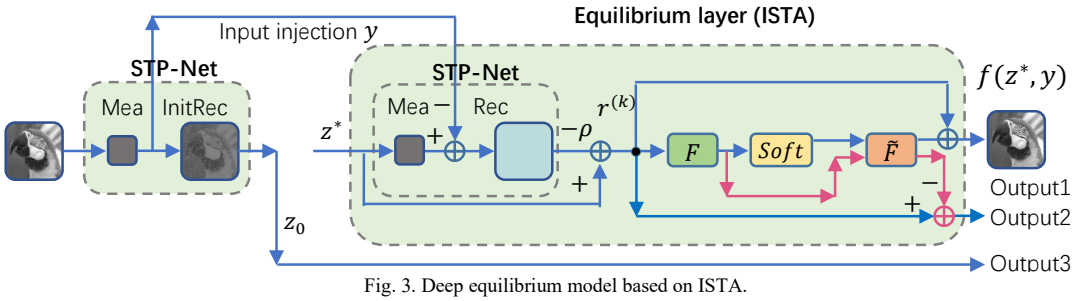

Fig. 3. Deep equilibrium model based on ISTA.

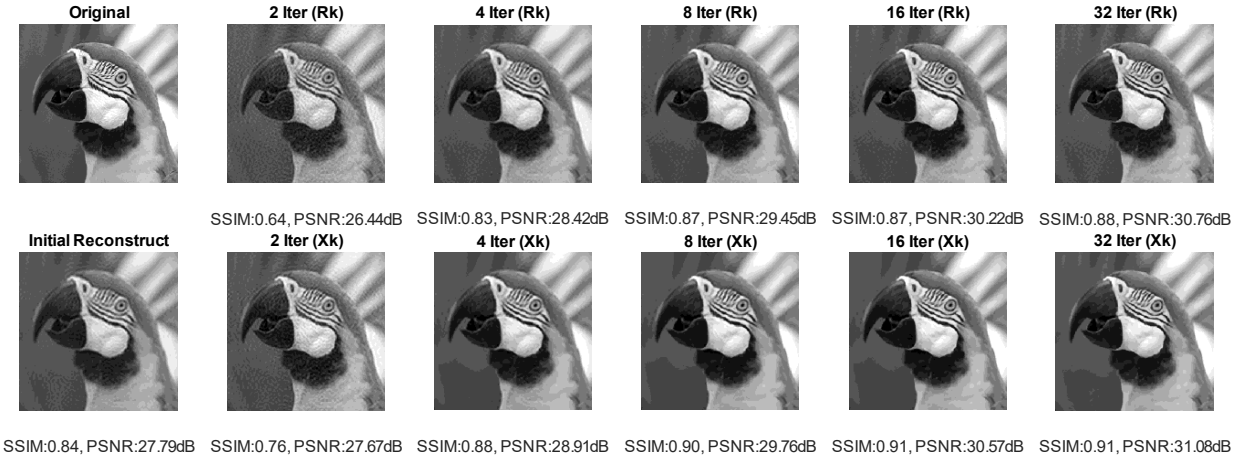

Fig. 4. Reconstruction results of parrot after specific ISTA iterations in STP-DEQ-Net (Sampling rate=10%)

A. ISTA for CS

Traditional image CS methods usually reconstruct an image by solving the optimization problem

$$x = \arg\min_x \frac{1}{2}\|y - \Phi x\|_2^2 + \lambda\|\Psi x\|_1 \tag{4}$$

where x is the vectorized original image, y is the measurements, Ψ denotes a sparse transform that is encouraged by the ℓ_1 -norm, and λ is a regularization parameter.

ISTA is a first-order proximal method which solves the problem by iteration of two steps

$$r^{(k)} = x^{(k-1)} - \rho\Phi^T\left(\Phi x^{(k-1)} - y\right) \tag{5}$$

$$x^{(k)} = \underset{x}{arg\,min}\,\frac{1}{2}\left\|x - r^{(k)}\right\|_2^2 + \lambda\|\Psi x\|_1 \tag{6}$$

where k is the iteration index and ρ is the step size [25]. $r^{(k)}$ is the immediate reconstruction result along the gradient descent direction of data-fidelity term $\frac{1}{2}\left\|\Phi x^{(k-1)} - y\right\|_2^2$ and $x^{(k)}$ is the output of every ISTA iteration [25].

Deep unrolling methods are state-of-the-art schemes that solve inverse problems by unrolling a small number of iterations of an iterative method, such as ISTA, alternating direction method of multipliers (ADMM) [29] and approximate message passing (AMP) [30]. It consists of several architecturally identical blocks. The number must be small since it is apt to run out of memory when training the network with more unrolled iterations [16].

B. STP-DEQ-Net

An equilibrium layer is applied in Fig. 3. A DEQ model is an approach corresponding to an infinite number of iterations. ISTA optimization can be modeled as an infinitely deep network with identical layers. For most deep layers the outputs actually converge to a fixed point (equilibrium point z^*) [16]

$$z^* = f(z^*, y) \tag{7}$$

where y is the input injection, z^* is input of the equilibrium layer, and f is the DEQ function. y is essential because the equilibrium point does not depend on z^*.

The key points here are computing the equilibrium output of the forward path and infer the fixed point of gradients in the backward path. Anderson acceleration method is a good choice for solving the problem [31]. For the gradients in the backward path, we deduce a new desired output, thereby producing updated gradients.

$$\tilde{O}_p = O_p - \left(\left(\frac{\partial f(z^*, y)}{\partial z^*}\right)^T \frac{(O_p - \tilde{O}_p)}{B} - g\right) B \tag{8}$$

where $\tilde{O}_p$ is the new desired output, O_p is the current output of ISTA block, B is mini-batch size, and g is the original gradients between loss function and output of the equilibrium layer. $\left(\frac{\partial f(z^*, y)}{\partial z^*}\right)^T \frac{(O_p - \tilde{O}_p)}{B}$ is the Jacobian-vector product which can be done via automatic differentiation tools. Then (8) is an implicit function that can be solved with Anderson acceleration method.

Fig. 3 shows the proposed STP-DEQ-Net. z_0 is the output of STP-Net which provides initial reconstruction as a starting

TABLE I. AVERAGE PSNR (DB) AND SSIM COMPARISONS ON SET11 AT DIFFERENT SAMPLING RATES

Algorithm	SR=1%		SR=4%		SR=10%		SR=25%	
	PSNR	SSIM	PSNR	SSIM	PSNR	SSIM	PSNR	SSIM
DPA-Net[20]	18.05	0.5011	23.50	0.7205	26.99	0.8354	31.74	0.9238
SSB-Net[21]	--	--	23.26	0.7000	27.49	0.8300	32.30	0.9200
DSCR-Net[22]	19.16	0.4811	22.53	0.6362	26.64	0.8328	29.41	0.9238
SWDGAN[23]	21.01	0.5410	24.67	0.6410	28.45	0.8570	33.45	0.9300
PENet[24]	20.74	0.4909	25.19	**0.7586**	28.58	**0.8701**	33.23	**0.9407**
ISTA-Net^{+}[25]	17.34	0.4131	21.31	0.6240	26.64	0.8036	32.57	0.9237
STP-Net	20.65	0.5053	23.39	0.6310	26.08	0.7679	30.06	0.8843
STP-ISTA-Net	**21.32**	0.5529	**25.47**	0.7152	**29.01**	0.8438	**33.72**	0.9327
STP-DEQ-Net	21.24	**0.5565**	24.67	0.7028	28.96	0.8495	32.63	0.9331

(ISTA-Net+ has 9 ISTA blocks. STP-ISTA-Net has 5 ISTA block. STP-DEQ-Net has 1 ISTA block. The best performance is labeled in bold.)

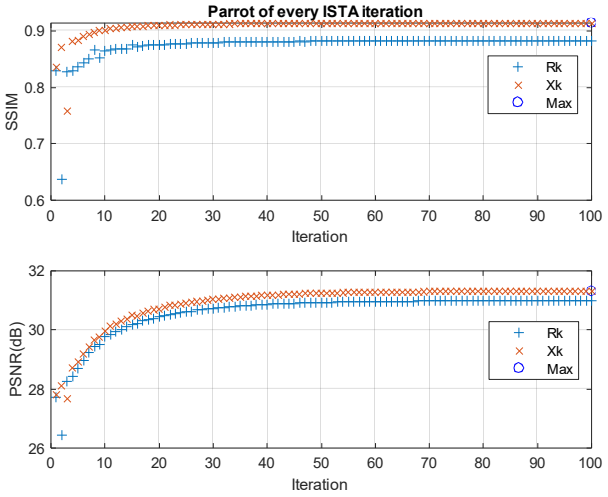

Fig. 5. Performance changes with ISTA iterations in STP-DEQ-Net (Sampling rate=10%)

point for equilibrium point computing. The loss function includes three parts. ISTA includes a sparse transform and its inverse transform, whose symmetry is constrained by Output2. Output3 and Output1 make the initial reconstruction and the output of the model approach to original image.

V. EXPERIMENTAL RESULTS

A. *Implementation details*

All the experiments are performed on a computer with Intel Core i7-8700K CPU, GeForce GTX1080 GPU and 16GB RAM. We use MATLAB R2020b to implement and train the STP-DEQ-Net separately for a range of sampling rates (1%, 4%, 10% and 25%). Natural images come from the ILSVRC2014 ImageNet dataset [32]. We extracted the central 256×256 part of each image and converted them to 8-bit grayscale. 20k images are selected: 14k for training, 3k for validation and 3k for testing. Training used stochastic gradient descent with momentum. For comparison, we also use 11 grayscale images (Set11) [33] during testing.

B. Proposed structures

Fig. 2 shows the structure of STP-Net [19]. It does CS sampling twice. For example, there is an image with size 256×256 and the sampling rate is 10%. Firstly, the image is measured row by row and every row produce 81 measurements. The second time the measurements are measured again along columns. Every column produce 81 measurements. So, the total sampling rate is $(81/256)^2 \approx 10\%$. The inverse process provides the initial reconstruction which can be a good choice for the subsequent networks. According to CS theory, the measurement operation should be linear, but

TABLE II. AVERAGE SSIM/PSNR COMPARISONS WITH DIFFERENT IMAGE CS METHODS ON 3K TESTING IMAGES AND SET11 (SR=10%)

Algorithm	3000 testing images		Set11	
	SSIM	PSNR (dB)	SSIM	PSNR (dB)
STP-Net	0.7555	26.66	0.7679	26.08
STP+1 ISTA Block	0.7494	27.05	0.7770	26.77
STP+5 ISTA Block (Same)	0.7645	27.63	0.8004	27.62
STP+5 ISTA Block (Diff)	0.7969	28.49	0.8438	29.01
STP+10 ISTA Block (Diff)	0.7991	**28.60**	**0.8514**	**29.32**
STP-DEQ-Net (10 Iter.)	0.8005	28.29	0.8294	28.24
STP-DEQ-Net (25 Iter.)	0.8039	28.35	0.8358	28.45
STP-DEQ-Net (50 Iter.)	**0.8058**	28.50	0.8495	28.96

(Same/Diff: every block has identical/different parameter values. The best performance is labeled in bold.)

the reconstruction process can be nonlinear. It means if convolutional layers are applied to implement the sampling process and the reconstruction process, the former should have no biases but the latter can contain biases.

We built STP-ISTA-Net first by connecting STP-Net with ISTA-Net. Since (5) has $\Phi^T\Phi x^{(k-1)}$ operation, STP-Net can be used repeatedly as measurement and reconstruction for each iteration. Our experiments adopt 5 ISTA iterations (blocks) and every convolutional layer uses 16 filters (each of size 3×3 in our experiments). Comparing with ISTA-Net introduced in [25] which has 9 ISTA blocks and every convolutional layer has 32 filters, our model is smaller. In Fig. 3, STP-DEQ-Net is built which only uses 1 ISTA block.

C. *Experimental* results

Fig. 4 shows the reconstructed image (parrot) after specific ISTA iterations in STP-DEQ-Net when sampling rate is 10%. The first row corresponds to (5) and the second row corresponds to (6). The figure shows repeated use of STP-DEQ-Net can improve the performance, which can also be observed in Fig. 5. Whether immediate reconstruction $r^{(k)}$ or output of the ISTA iteration $x^{(k)}$, their qualities are all improved with more iterations, and the quality of $x^{(k)}$ is a little better than $r^{(k)}$. The phenomenon is different with deep unrolling methods such as ISTA-Net. The trained ISTA-Net could not be repeatedly used to implement more ISTA iterations because it will have significant degradation[16].

Table I shows the average performance comparison on Set11 at different sampling rates for various algorithms. It shows STP-ISTA-Net has higher PSNR than other algorithms, since STP-Net provides a good initial reconstruction for it. Though STP-DEQ-Net has much fewer learnable parameters than STP-ISTA-Net, it still has competitive performance. PENet shows its high SSIM since it contains a basic network and an enhanced network that is specially designed for acquiring details. In Table II, the reconstruction results of STP-Net display high PSNR and SSIM. This means STP-Net

can capture useful information effectively. At the same time, though the table shows STP-DEQ-Net has reasonable performance with repeated use for multiple ISTA iterations, PSNR of the restored images is lower than STP-ISTA-Net with 10 ISTA blocks. The number of learnable parameters in the former is only one-tenth that in the latter. It confirms that a network with more learnable parameters is more powerful since STP-DEQ-Net has only one block of ISTA structure.

VI. Conclusion

Inspired by the ISTA algorithm and DEQ model, we present STP-DEQ-Net. The trained model can be repeatedly used to implement more iterations and yield a consistent improvement in reconstruction quality. It has much fewer learnable parameters than other deep unrolling methods but it has trade-offs between reconstruction quality and computation. The model merges the merits of traditional optimization method and novel network method. Compared with other network-based CS reconstruction methods, our model is simple and the structure has better interpretability.

Acknowledgment

This research was partially funded through a grant from the Natural Sciences and Engineering Research Council (NSERC) of Canada.

References

[1] E. J. Candes and J. K. Romberg, "Signal recovery from random projections," *Computational Imaging III*, vol. 5674, no. March 2005, pp. 76–86, 2005, doi: 10.1117/12.600722.

[2] R. G. Baraniuk, V. Cevher, and M. F. Duarte, "Model-based compressive sensing," *IEEE Transactions on information theory*, vol. 56, no. 4, pp. 1982–2001, 2010.

[3] D. L. Donoho, "Compressed sensing," *IEEE Transactions on Information Theory*, vol. 52, no. 4, pp. 1289–1306, 2006, doi: 10.1109/TIT.2006.871582.

[4] E. J. Candès, J. Romberg, and T. Tao, "Robust uncertainty principles: Exact signal reconstruction from highly incomplete frequency information," *IEEE Transactions on Information Theory*, vol. 52, no. 2, pp. 489–509, 2006, doi: 10.1109/TIT.2005.862083.

[5] E. J. Candès, J. K. Romberg, and T. Tao, "Stable signal recovery from incomplete and inaccurate measurements," *Communications on Pure and Applied Mathematics*, vol. 59, no. 8, pp. 1207–1223, 2006, doi: 10.1002/cpa.20124.

[6] A. M. Assem and R. M. Dansereau, "Compressive sensing using S-transform in pulse radar," *2017 40th International Conference on Telecommunications and Signal Processing, TSP 2017*, vol. 2017-Janua, pp. 488–492, 2017, doi: 10.1109/TSP.2017.8076034.

[7] P. Firoozi, S. Rajan, and I. Lambadaris, "Efficient Kronecker-based sparse one-time sensing matrix for compressive sensing cryptosystem," *2021 IEEE Intern. Mediterranean Conf. on Communications and Networking, MeditCom 2021*, pp. 354–359, 2021.

[8] J. Huang and F. Yang, "Compressed magnetic resonance imaging based on wavelet sparsity and nonlocal total variation," *2012 9th IEEE Intern. Symposium on Biomedical Imaging (ISBI)*, pp. 968–971, 2012.

[9] B. Huang, X. Yan, J. Zhou, and Y. Fan, "CSMCNet: Scalable video compressive sensing reconstruction with interpretable motion estimation," pp. 1–12, 2021, [Online]. Available: http://arxiv.org/abs/2108.01522

[10] Y. Liu, X. Yuan, J. Suo, D. J. Brady, and Q. Dai, "Rank minimization for snapshot compressive imaging," *IEEE Transactions on Pattern Analysis and Machine Intelligence*, vol. 41, no. 12, pp. 2990–3006, 2019, doi: 10.1109/TPAMI.2018.2873587.

[11] E. J. Candes and T. Tao, "Decoding by linear programming," *IEEE Transactions on Information Theory*, vol. 51, no. 12, pp. 4203–4215, 2005, doi: 10.1109/TIT.2005.858979.

[12] Y. Yu and R. M. Dansereau, "Fast reconstruction of 1D compressive sensing data using a deep neural network," *International Journal of Signal Processing Systems (IJSPS)*, vol. 8, no. 1, pp. 26-31, March 2020. doi: 10.18178/ijsps.8.1.26-31.

[13] R. H. M. Rafi and A. C. Gurbuz, "Data driven measurement matrix learning for sparse reconstruction," *2019 IEEE Data Science Workshop, DSW 2019 - Proceedings*, pp. 253–257, 2019.

[14] V. Monga, Y. Li, and Y. C. Eldar, "Algorithm unrolling: Interpretable, efficient deep learning for signal and image processing," *IEEE Signal Processing Magazine*, vol. 38, no. 2, pp. 18–44, 2021.

[15] S. Bai, J. Zico Kolter, and V. Koltun, "Deep equilibrium models," *arXiv*, no. NeurIPS, 2019.

[16] D. Gilton, G. Ongie, and R. Willett, "Deep equilibrium architectures for inverse problems in imaging," *IEEE Transactions on Computational Imaging*, vol. 7, pp. 1123–1133, 2021, doi: 10.1109/TCI.2021.3118944.

[17] J. Wang, S. Ye, Y. Ruan, and C. Chen, "Low storage space for compressive sensing: semi-tensor product approach," *Eurasip Journal on Image and Video Processing*, vol. 2017, no. 1, pp. 1–13, 2017, doi: 10.1186/s13640-017-0199-9.

[18] J. Wang, Z. Xu, Z. Wang, S. Xu, and J. Jiang, "Rapid compressed sensing reconstruction: A semi-tensor product approach," *Information Sciences*, vol. 512, pp. 693–707, 2020, doi: 10.1016/j.ins.2019.09.071.

[19] Y. Yu and R. M. Dansereau, "STP-Net: Semi-tensor product neural network for image compressive sensing," *Intern. Conf. on Advances in Signal, Image and Video Process.*, no. 2, pp. 7–12, 2022.

[20] Y. Sun, J. Chen, Q. Liu, B. Liu, and G. Guo, "Dual-path attention network for compressed sensing image reconstruction," *IEEE Transactions on Image Processing*, vol. 29, pp. 9482–9495, 2020, doi: 10.1109/TIP.2020.3023629.

[21] T. Pang, Y. Quan, and H. Ji, "Self-supervised Bayesian deep learning for image recovery with applications to compressive sensing," *European Conference on Computer Vision 2020*, no. Aug, pp. 475–491, 2020, doi: 10.1007/978-3-030-58621-8_28.

[22] Z. Zheng *et al.*, "DSCR-NET: A diffractive sensing and complex-valued reconstruction network for compressive sensing," *Proceedings - IEEE International Symposium on Circuits and Systems*, vol. 2020-Octob, 2020, doi: 10.1109/iscas45731.2020.9181225.

[23] Y. Tian, X. Chai, Z. Gan, Y. Lu, Y. Zhang, and S. Song, "SWDGAN: GAN-based sampling and whole image denoising network for compressed sensing image reconstruction," *J. Electronic Imaging*, vol. 30, no. 06, pp. 1–22, 2021, doi: 10.1117/1.jei.30.6.063017.

[24] W. Ma and X. Wu, "Parallel enhanced network for image compressed sensing," *InInternational Conference on Image, Signal Processing, and Pattern Recognition (ISPP 2022)*, vol. 12247, no. Apr, pp. 73–77, 2022, doi: 10.1117/12.2636940.

[25] J. Zhang and B. Ghanem, "ISTA-Net: Interpretable optimization-inspired deep network for image compressive sensing," *Proc. of the IEEE Computer Society Conference on Computer Vision and Pattern Recognition*, pp. 1828–1837, 2018, doi: 10.1109/CVPR.2018.00196.

[26] L. Gan, "Block compressed sensing of natural images," *2007 15th International Conference on Digital Signal Processing, DSP 2007*, no. 1, pp. 403–406, 2007, doi: 10.1109/ICDSP.2007.4288604.

[27] X. Xie, C. Wang, J. Du, and G. Shi, "Full image recover for block-based compressive sensing," *Proceedings - IEEE International Conference on Multimedia and Expo*, vol. 2018-July, pp. 2–7, 2018.

[28] H. Qi and D. Cheng, "Analysis and control of Boolean networks: A semi-tensor product approach," *7th Asian Control Conference*, vol. 37, no. 5, pp. 1352–1356, 2009, doi: 10.3724/SP.J.1004.2011.00529.

[29] Y. Yang, J. Sun, H. Li, and Z. Xu, "Deep ADMM-Net for compressive sensing MRI," *Advances in Neural Information Processing Systems*, no. Nips, pp. 10–18, 2016.

[30] N. Li and C. C. Zhou, "AMPA-Net: Optimization-inspired attention neural network for deep compressed sensing," *International Conf. on Communication Technology Proceedings, ICCT*, vol. 2020-Octob, pp. 1338–1344, 2020, doi: 10.1109/ICCT50939.2020.9295956.

[31] D. Duvenaud, J. Z. Kolter, and M. Johnson, "Deep implicit layers: Neural ODEs, equilibrium models, and beyond," *NeurIPS workshop*, 2020. http://implicit-layers-tutorial.org/

[32] O. Russakovsky *et al.*, "ImageNet large scale visual recognition challenge," *International Journal of Computer Vision*, vol. 115, no. 3, pp. 211–252, 2015, doi: 10.1007/s11263-015-0816-y.

[33] K. Kulkarni, S. Lohit, P. Turaga, R. Kerviche, and A. Ashok, "ReconNet: Non-iterative reconstruction of images from compressively sensed measurements," *Proc. of the IEEE Computer Society Conference on Computer Vision and Pattern Recognition*, vol. 2016-Decem, pp. 449–458, 2016, doi: 10.1109/CVPR.2016.55.